ORIGINAL PAPER

Chun-Guey Wu · Hu Leng Lin · Nai-Ling Shau

Magnetic nanowires via template electrodeposition

Abstract The magnetic $NiFe_x$ nanowires were prepared via template-guided electrodeposition. Anodized nanoporous aluminum was used as a template. The pore density and dimensions of alumina templates can be controlled by anodization conditions. Magnetic nanorods (or nanowires) with various aspect ratios were prepared by controlling the electrodeposition time. SEM and TEM micrographs revealed the wire and rod shape morphologies with 50 nm in diameter and $1.5 \sim 10$ μm in length. Elemental analysis and ESCA studies suggested that $NiFe_3$ magnetic alloy was formed. The X-ray diffraction pattern indicates that all the nanowires are stabilized in a BCC structure with a [1 1 0] texture oriented along the long axis of the nanowires. The magnetic measurement showed no hysteresis loops for the whole aspect ratios of the nanowires. Nevertheless, the magnetization is more temperature sensitive for nanowires with lower aspect ratio. This is caused by the fact that the easy magnetization axis is always parallel to the long axis of the nanowires.

Keywords Template · AAO · Permalloy · Magnetization · Electrodeposition

Introduction

Nanosicence and technology are the terms used to describe the creation and exploitation of materials with structural features in between those of atoms and bulk materials. The attraction of the nanostructured materials stems from the fact that their properties may be different from the corresponding bulk materials. For example, the magnetic property of Fe powder with a crystallite size of 13 nm showed a coercivity of 900 Oe in comparison with 10 Oe for bulk Fe [1].

Nanoscale patterned magnet arrays have also been suggested as recording media to achieve the recording densities of more than 100 Gbit/in^2 [2, 3]. Many magnetic nanowire arrays of metal [4–6], alloy [7, 8], or multilayer structure [9, 10] have been studied. Amongst the materials studied, permalloy (Fe–Ni alloy) is widely attractive because of its high magnetization behavior and invar effect in certain compositions [11, 12]. On the other hand, electrochemical synthesis method is suitable for deposition of nanowires in nanometer-wide cylindrical pores of porous materials [13–22]. When magnetic metals are electrodeposited into these pores, the magnetic properties of the nanowire are already conferred.

In the present article, the template electrodeposition method was used to prepare $NiFe_3$ nanowires with various aspect ratios. The template used was anodized aluminum foil (AAO). The as-prepared nanowires were extracted from the template by removing the AAO with an alkali solution. The pure magnetic nanowires (free of template) were well-characterized and the magnetic properties were studied.

Experiment section

Materials Aluminum foil (99.99%, 0.1 mm thick) was cleaned with a detergent and then rinsed with copious amounts of water. $H_2C_2O_{4(aq)}$, $H_3PO_{4(aq)}$, $FeSO_4$, $NiSO_4$, $H_3BO_{3(aq)}$, and NaOH were obtained from the commercial resources and used without further purification.

Preparation of AAO template The one-step anodized alumium oxide template was prepared followed the literature report [23, 24] with slight modification. The high purity (99.99%) Al foil is degreased and cut into a 2.5 cm × 10 cm strip, then annealed at 500°C for 4 h under N_2. The clean Al foil was DC anodized in 0.3 M $H_2C_2O_{4(aq)}$ at 40 V (DC) for 1 h to form a porous alumina template

C.-G. Wu (✉) · H. L. Lin · N.-L. Shau
Department of Chemistry, National Central University,
Chung-Li, Taiwan, 32054, ROC
E-mail: t610002@cc.ncu.edu.tw
Tel.: +886-3-4227151ext 65903
Fax: +886-3-4227664

with pore diameter of 50 nm. The aluminum oxide barrier layer was removed with a 5% $H_3PO_{4(aq)}$ for 30 s, washed with distilled water, and then dried in air.

Electrochemical deposition of Ni–Fe alloy For the template electrodeposition of Ni-Fe nanowires, the anodized alumium template was used as a working electrode. Electrochemical deposition was performed in a single-compartment, three-electrode cell with an Ni foil counter electrode and an Ag/AgCl reference electrode. The supporting electrolyte was 0.5 M $FeSO_{4(aq)}$/0.5 M $NiSO_{4(aq)}$/0.3 M $H_3BO_{3(aq)}$. High concentration (0.5 M) of $FeSO_{4(aq)}$ and $NiSO_{4(aq)}$ were used to maintain constant ion migration rate. The electrodeposition was carried out with a constant potential (chronoamperometric, −1.0 V vs SCE) using an Autolab potentiostat/galvanostat. The deposition times used were: 100 s, 600 s, and 40 min. The length of the Ni–Fe nanowires was dependent of the deposition time.

Extracting the nanowires from the AAO templates The Ni–Fe nanowires were separated from the anodic aluminum oxide (AAO) template by dissolving the template with Ni–Fe nanowires in a 5% NaOH aqueous solution. A magnetic field was applied under the bottom of the container to assist the precipitation of Ni–Fe nanowires and a pipette was used to withdraw the solution waste. The template free Ni–Fe nanowire was washed with distilled water several times and dried under vacuum.

Physicochemical measurements Scanning Electron Microscopy (SEM) and Energy Dispersive Spectroscopy (EDS) studies were done with Hitachi S-800 at 15 kV. Transmission Electron Micrograph (TEM) was taken with JEOL JEM-2000FXII at the acceleration voltage of 160 kV. X-ray powder diffraction studies were carried out with a Shimadzu XRD-6000 X-ray diffractometer using Cu–Kα radiation at 30 kV and 30 mA. X-ray photoelectron spectroscopy studies were carried out on a Perkin-Elmer PHI-590AM ESCA/XPS spectrometer system with a Cylindrical Mirror Electron (CMA) energy analyzer. The X-ray sources were Al Kα at 600 W and Mg Kα at 400 W. The iron and nickel contents are examined by atomic absorption spectrometry and ESCA analysis. The magnetic properties are measured using an Omega 6000 PPMS system.

Results and discussion

The preparation of Anodic Aluminum oxide (AAO) template [25, 26]

A hexagonal array of nanometer-sized pores was formed in annealed aluminum foil after anodizing at 40 V for one hour in 0.3 M $H_2C_2O_4$ aqueous solution as shown in Fig. 1. The diameter of the pore is about 50 nm and the distance between the pores is close to 100 nm. If the clean aluminum was anodized without annealing first,

no ordered hexagonal pores were found. The annealing process reduced the stress of Al foil and formed a hexagonal domain for the formation of regular pores. The length of anodized aluminum template was controlled with the anodization time and conditions. When the Al foil was anodized for 1 h, nanopores with lengths longer than 10 μm were fabricated. The alumina barrier layer of the as-prepared AAO template was removed by dipping the template in a 5% $H_3PO_{4(aq)}$ for 30 s and then washing with copious amounts of water. We keep a layer of unanodized Al metal on purpose, since the conducting Al metal was used as electrode surface for electrochemical deposition of the Ni–Fe alloy.

Template electrodeposition of Ni–Fe nanowires and extract the Ni–Fe nanowires from the AAO template

Ni–Fe nanowires were prepared using an electrochemical deposition from the corresponding ions, Ni^{+2} and Fe^{+2}. The stoichiometry and aspect ratio of Ni–Fe nanowires were significantly affected by the plating temperature, agitation conditions, ionic characteristics, pH, pulse current, and additives [27]. Therefore, in this study, we used the chronoamperometry method and carefully controlled all the experimental parameters to be the same, except the deposition time. A high concentration (in our experiment, the concentration of Ni^{+2} and Fe^{+2} we used in this study is 0.5 M, higher than that used in metal plating) of Ni and Fe sources were used to maintain constant ion migration rate and avoid the change of concentration that may affect the stoichiometry of the Ni–Fe nanowires. The current-time curve at applied voltage of −1.0 V (vs SCE) is shown in Fig. 2. In the beginning of deposition, the current increased slightly, indicating the filling of the pores. When all the pores were full, deposition occurred on the whole surface of AAO template, and the current increased abruptly. The current–time curve showed that it takes ca. 1,300 s to fill the pores of the AAO template we made. Therefore three deposition times, 100 s, 600 s and 2,400 s, were used to synthesize the Ni–Fe nanowires with different aspect ratio.

To extract the Ni–Fe nanowires from the AAO template, several acidic and basic solutions, such as $H_2SO_{4(aq)}$, $H_3PO_{4(aq)}$, $H_2C_2O_{4(aq)}$ and $NaOH_{(aq)}$ were used to dissolve the alumina wall of AAO template
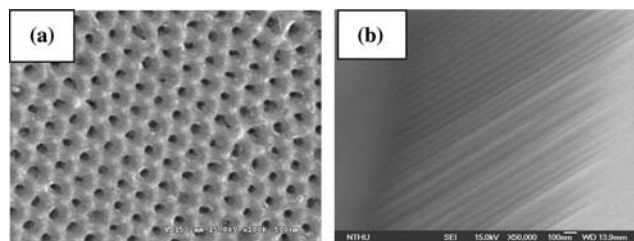

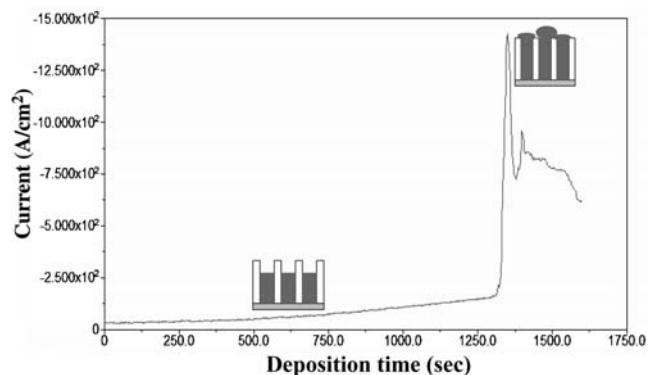**Fig. 1** SEM images of AAO template. **a** Top-view (100,000x) **b** Cross- section view (50,000×)

Fig. 2 The current-time curve for the template electrodeposition of Ni–Fe nanowire

Fig. 4 XRD pattern of NiFe$_3$ nanowires

Table 1 The atomic ratios of Fe and Ni obtained from the ESCA and Atomic absorption analysis

Analysis method		Fe (atomic%)	Ni (atomic%)
ESCA analysis	Spot 1	72.7	27.3
	Spot 2	77.7	22.3
	Spot 3	72.6	27.4
	Average	74.3	25.7
Atomic absorption analysis		73.5	26.5

(Alumina (Al$_2$O$_3$) is an amphoteric material). However, we found that Ni–Fe nanowires as well as alumina walls dissolved in acidic solution. If the basic solution such as NaOH$_{(aq)}$ was used, both alumina and aluminum in the AAO template were dissolved, but not Ni–Fe nanowires. Therefore, pure Ni–Fe nanowires can be collected by the assistance of a magnet. The Ni–Fe nanowires were washed with distilled water several times and dried under vacuum.

Characterization of Ni–Fe nanowires

The composition of the Ni-Fe nanowires was estimated to be Ni$_{0.25}$Fe$_{0.75}$ (or NiFe$_3$) using ESCA and atomic absorption analysis, and the results were listed in Table 1. ESCA analysis was performed on the NiFe$_3$ pellet (the nanowires were pressed into a pellet). The atomic ratio of Ni to Fe was calculated from the integral of the ESCA signal and further calibrated with the sensitivity factor of the instrument. Furthermore,
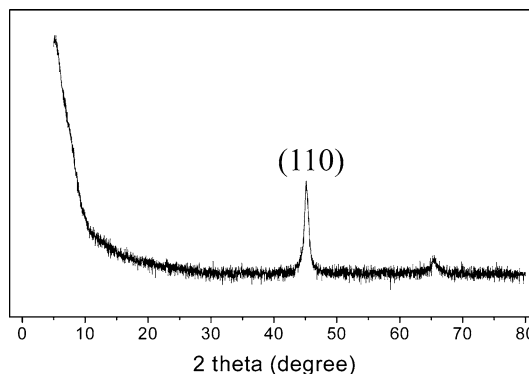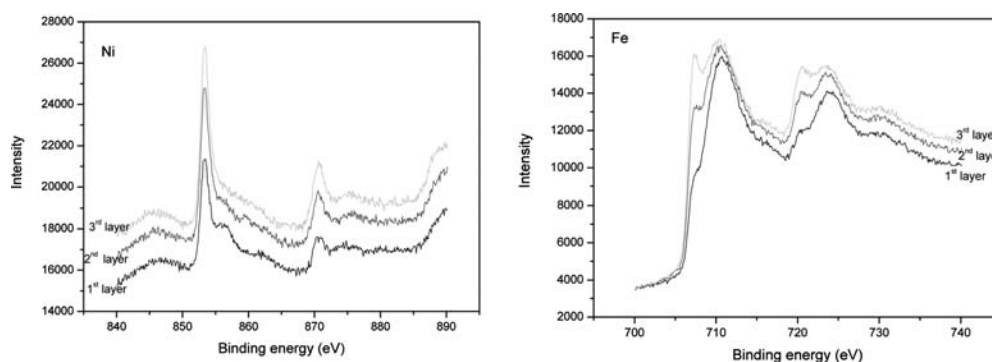
depth-profile ESCA analysis (Fig. 3, the first layer is 18 nm in depth from the surface of the pellet; the second and the third layers are 48 nm and 78 nm in depth from the surface of the pellet, respectively) revealed that the atomic ratios of Fe and Ni were very similar through the whole thickness of the pellet. These results suggested that the composition of individual nanowire could be similar to each other. They are alloy, not simple metal mixture. The structure of the Ni-Fe nanowires was identified with an X-ray diffraction (see Fig. 4). There are two diffraction peaks appeared at 2θ from 2 to 80°. The domain size of NiFe$_3$ nanowires was estimated to be 50 ∼ 70 nm using a Scherr's equation. The diffraction data is consistent with the assumption that each NiFe$_3$ nanowire is a single crystal. Attempts to probe the structure of single NiFe$_3$ nanowires with electron diffraction was fail, due to the thermal instability of the NiFe$_3$ nanowires. They formed aggregates when the high energy (160 KV) electron beam was focus on the nanowires.

The morphology of the NiFe$_3$ nanowires was revealed with the SEM and TEM micrographs. The SEM images (Fig. 5) showed that the average diameter of the NiFe$_3$ nanowires is 50 nm and the length is larger than 2 μm. The diameter of the nanowires is consistent with the pore size of the AAO template. The NiFe$_3$ nanowires are fragile, and they broke during the isolating process. Therefore, it is difficult to estimate their length from the SEM micrographs. The surface of the NiFe$_3$ nanowires shown in Figure 5 is smooth, suggesting that the wall of AAO template is also very flat.

Fig. 3 Depth profile ESCA spectra of the pellet of NiFe$_3$ nanowires

Fig. 5 SEM micrographs of NiFe₃ nanowires prepared from different electrochemical deposition time. **a** 2,400 s (NF2400). **b** 600 s (NF600)
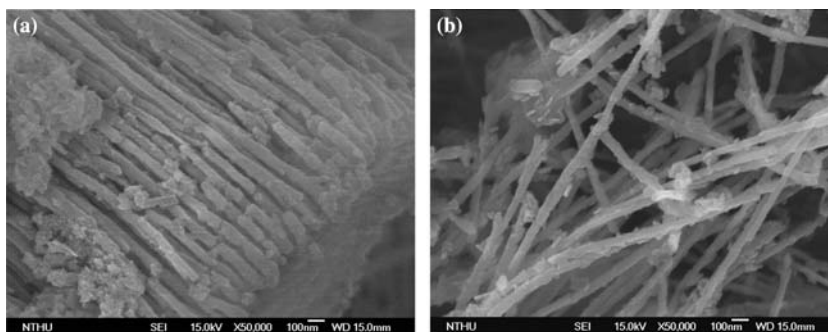
Figure 6 displayed the dark field TEM images of the nanowires obtained from different deposition times. The apparent diameter of the nanowires is close to that revealed by SEM images. Interestingly, we found that these NiFe₃ nanowires tend to get together to form a bundle-like structure, probably due to the fact that they are tiny magnets. The magnetic interaction causes the magnetic nanowires to aggregate. The dimensions of NiFe₃ nanowires obtained from different electrochemical deposition times were listed in Table 2.

Magnetic characterization

The NiFe₃ nanowires can be regarded as tiny magnets; they are very sensitive to magnetic fields. When small amount of FN600 nanowires was suspended in ethanol,

Fig. 6 Dark field TEM images of NiFe₃ nanowires **a**, **b** NF2400, **c** NF600. **d** NF100 (obtained from the 100 s electrochemical deposition)

they dispersed randomly in the solvent as shown in Fig. 7a. Nevertheless, when a weak magnetic field was applied (by placing a small magnet, not shown in the photograph, on the back of the container), the NiFe₃ nanowires start to gather and assemble into an ordered pattern (the long axis of the NiFe₃ nanowires aligned toward the magnet, see Fig. 7b). By increasing the magnetic field (moving the magnet close to the container), the NiFe₃ nanowires get closer to each other and also aligned with their long axis toward the magnet (Fig. 7c). These phenomena suggested that the spin orientation of these NiFe₃ nanowires is along the long axis. The high sensitivity toward the magnetic field gives NiFe₃ nanowires have a great potential for use in disease diagnosis and treatment.

The magnetization of NiFe₃ nanowires with different aspect ratio was measured with a PPMS measuring system. The magnetization loops of NiFe₃ nanowires in two aspect ratios were shown in Fig. 8. No observable hystersis loop suggested that NiFe₃ nanowires of both aspect ratios have a reversible magnetization behavior. Nevertheless, the magnetization depends on the aspect ratio of the nanowires. The saturated magnetization of nanowires with bigger aspect ratio is also higher (320 vs. 231 emu/g for nanowires with 10 μm and 5 μm in length respectively), consistent with the spin is aligned along the long axis of the magnetic nanowire. Furthermore, the magnetization is more temperature sensitive for NiFe₃ nanowire with lower aspect ratio. This is also due to the fact that the easy magnetization axis is always parallel to the long axis of the nanowires. The detailed studies of the magnetic properties of these magnetic nanowires are in progress.
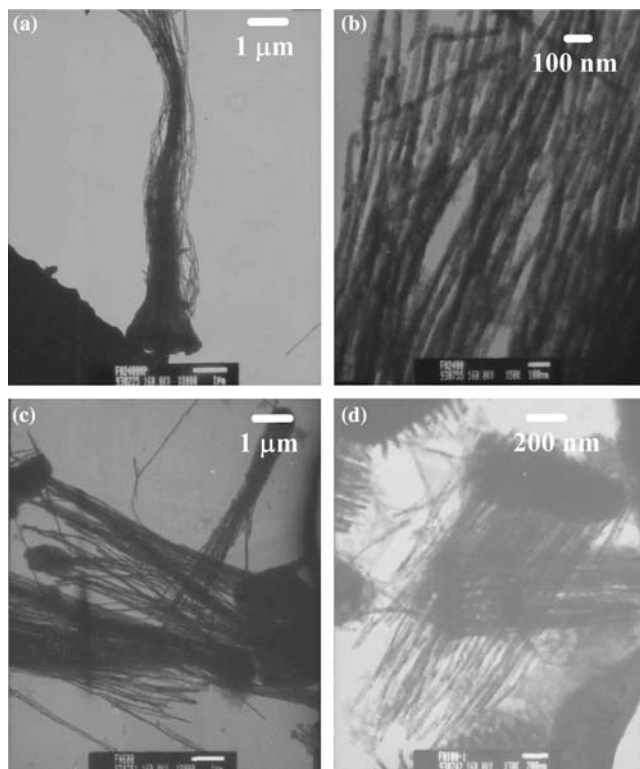
Conclusion

NiFe₃ alloy nanowires were fabricated in the nanochannels of AAO by electrochemical deposition. SEM and

Table 2 The dimensions of the NiFe₃ nanowires obtained from various electrochemical deposition times

Deposition time	Diameter (D, nm)	Length (L, nm)	Aspect ratio (L/D)
40 min (NF2400)	50	10000	200
10 min (NF600)	50	5000	100
100 s (NF100)	50	1500	30

Fig. 7 The photographs of FN600/ethanol solution: **a** without magnetic field, **b** under weak magnetic field, **c** under strong magnetic field
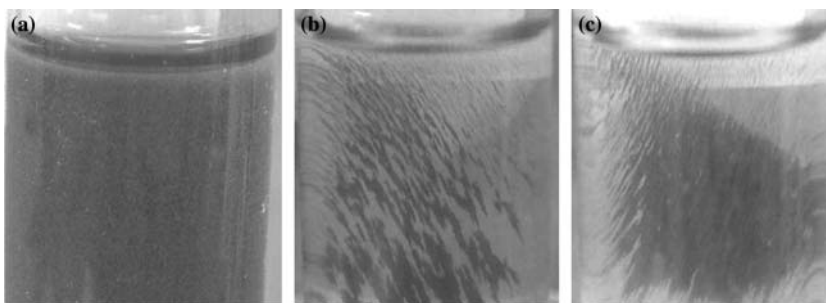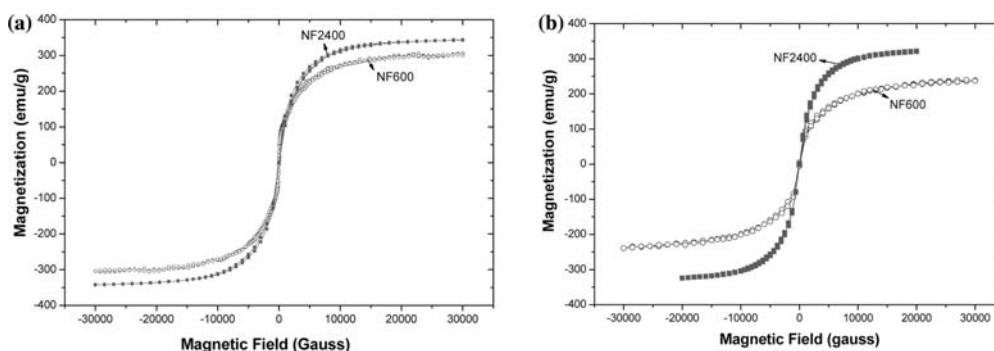

Fig. 8 Hysteresis loops for two NiFe$_3$ nanowires at two temperatures **a** 10 K **b** 300 K

TEM micrographs revealed that these magnetic nanowires are 50 nm in diameter and 1.5 ∼ 10 μm in length, depending on deposition time. Magnetic measurements suggested that NiFe$_3$ nanowires are ferromagnetic, and that the magnetization and temperature-dependent magnetic properties depend on the aspect ratios of the nanowire. The high sensitivity toward the magnetic field gives these magnetic nanowires have a great potential for use in the disease diagnosis and treatment.

References

1. Gangopadhyay S, Hadjipanayis S, Kostikas A (1992) Phys Rev B 45:9778
2. Shen J, Skomski R, Klaua M. Jenniches H, Manoharan SS, Kirschner J (1997) Phys Rev B 56:2340
3. Wang YW, Zhang LD, Meng GW, Peng XS, Jin YX, Zhang J (2002) J Phys Chem B 106:2502
4. Peng Y, Zhang HL, Pan SL, Li HL (2000) J Appl Phys 87:7405
5. Zeng M, Menon L (2000) Phys Rev B 62:12282
6. Dubois S, Colin J, Duvail JL, Piraux L (2000) Phys Rev B 61:14315
7. Li F, Ren L (2002) Phys Stat Sol 193:196
8. Szabo S, Kis-Varga M, Beke DL, Juhasz RJ (2000) Magn Magn Mater 60–62:215
9. Guo Y, Wan LJ, Bai CL (2003) Chem Mater 15:664
10. Piraux L, Dubois S, Duvail JL (1997) J Magn Magn Mater175:127
11. Khan HR, Petrikowski K (2000) J Magn Magn Mater 213:526
12. Zhu H, Yang SG, Ni G, Tang SL, Du YW (2001) J Phys: Condens Matter 13:1727
13. Lodder JC, Cheng-Zhang L (1989) IEEE Trans Magn 25:4171
14. Arai KI, Ishiyama K, Ohoka Y, Kang HW (1989) J Magn Soc Japan 13:789
15. Mawlawi D Al, Coombs N, Moskovits M (1991) J Appl Phys 70:4421
16. Whitney TM, Jiang JS, Searson PC, Chien CL (1993) Science 261:1316
17. Masuda H, Fukuda K (1995) Science 268:1466
18. Masuda H, Satoh M (1996) Jpn J Appl Phys 35:L126
19. Li AP, Müller F, Birner A, Nielsch K, Gösele U (1998) J Appl Phys 84:6023
20. Li AP, Müller F, Birner A, Nielsch K, Gösele U (1999) J Vac Sci Technol A 17:1428
21. Asoh H, Nishio K, Nakao M, Yokoo A, Tamamura T, Masuda H (2001) J Vac Sci Technol B 19:569
22. Xu T, Zangari G, Metzger RM (2002) Nano Lett 2:37–41
23. Wang X, Han GR (2003) Microelectro Eng 66:166
24. Schmid GJ (2002) Mater Chem 12:1231
25. Wang X, Han GR (2003) Microelectro Eng 66:166
26. Schmid G (2002) J Mater Chem 12:1231
27. Tsay P, Hu C C (2002) J Electrochem Soc 149(10): C492